



Research Article

Revisiting the Serviceability of Long-Span Bridges under Vortex-Induced Vibrations Based on Human Body Vibration

Jingxi Qin,¹ Jin Zhu ,^{2,3} Han Li,² Ziluo Xiong ,² and Yongle Li^{2,3}

¹Department of Civil and Environmental Engineering, University of California, Los Angeles, CA 90095, USA

²Department of Bridge Engineering, Southwest Jiaotong University, Chengdu, Sichuan 610031, China

³State Key Laboratory of Bridge Intelligent and Green Construction, Southwest Jiaotong University, Chengdu, Sichuan 611756, China

Correspondence should be addressed to Jin Zhu; zhujin19880102@126.com and Ziluo Xiong; ziluoXiong@my.swjtu.edu.cn

Received 19 August 2023; Revised 4 February 2024; Accepted 7 February 2024; Published 23 February 2024

Academic Editor: Mohamed Ichchou

Copyright © 2024 Jingxi Qin et al. This is an open access article distributed under the Creative Commons Attribution License, which permits unrestricted use, distribution, and reproduction in any medium, provided the original work is properly cited.

Vortex-induced vibrations (VIVs) have been frequently observed on long-span bridges (LSBs) in recent years. Unlike other destructive aerodynamic phenomena of LSBs, VIVs are self-limited in amplitude, primarily affecting the serviceability of LSBs through unpleasant users' feelings characterized by human body vibration. Most existing studies discussed this issue based on a popular human body vibration measure, the human comfort index (HCI) in ISO 2631-1. However, the HCI is primarily concerned with vibration above 0.5 Hz, which might be unsuitable for disclosing the influence of VIV because of the low-frequency features of LSBs' VIVs. To address this limitation, this study advocates using the motion sickness index (MSI) to revisit the serviceability of LSBs experiencing VIVs based on an innovative wind-traffic-bridge simulation platform. Different from current studies exclusively focusing on vehicle riders, this paper additionally incorporates a vibration model for standing persons to understand the feelings of the pedestrians on the bridge. On this basis, the influence of VIV and traffic load is comprehensively examined. The results indicate that the HCI is inappropriate for exploring the serviceability of LSBs under VIVs regarding users' feelings, but the MSI is a good alternative. Moreover, the increasing traffic load can obviously mitigate the adverse effect of VIVs on the bridge's serviceability, which may be utilized to control VIVs of LSBs in real-world engineering practice.

1. Introduction

The rapid development of high-strength materials and construction technology has promoted the emergence of long-span bridges (LSBs) worldwide. The inherent characteristics of high flexibility and low structural damping of LSBs render them highly susceptible to aeroelastic phenomena, such as vortex-induced vibration (VIV), coupled flutter, torsional flutter, and galloping [1]. VIVs usually occur at modest wind environments (i.e., relatively low wind speeds), and the resulting aerodynamic forces acting on the bridge deck make the VIV self-limited in amplitude. For the other three typical aerodynamic phenomena, the bridge vibration amplitude tends to increase continuously and, therefore, can lead to aeroelastic instabilities [2]. As a result, the VIV is commonly deemed less destructive than the other

three and a potential serviceability threat for LSBs [3, 4]. Unfortunately, VIVs have been frequently observed on LSBs in recent years. Typical examples include the Trans-Tokyo Bay crossing bridge in Japan [5], Ewijk bridge in Netherlands [6], and Volgograd continuous bridge in Russia [7]. Notably, two VIV events appeared successively on the Yingwuzhou Yangtze River Bridge [8] and Humen Bridge [9] in one week. The field inspection and theoretical analysis suggested that the oscillations (i.e., VIVs) on the above two bridges caused trivial structural deterioration/damage, but the oscillations make some people unpleasant when using the bridges [10, 11]. In particular, the VIV amplitude of Humen Bridge was so noticeable that the bridge managers promptly shut down the bridge for 10 days until no obvious VIVs to prevent bridge users from unpleasant feelings [12]. Although closing the bridge is an effective way to avoid

serviceability concerns, it is an expedient countermeasure and kind of overconservative. This makeshift adversely influenced traffic mobility, which is unfavorable for a traffic bottleneck like a LSB. Actually, the deficient understanding of bridge users' feelings about VIVs, i.e., whether it is pleasant for bridge users to travel on the bridge under a specific VIV, is blamed for this conduct. Therefore, a reliable evaluation framework of the serviceability of LSBs under VIVs is needed to be prepared for any future possible VIVs.

To ensure good serviceability, many bridge design codes and standards have established serviceability limit states for LSBs under VIVs, such as the AASHTO [13], Chinese code [14], and Japanese guide [15]. However, most codes and standards were formulated in a very crude manner, which may be inadequate to meet the current requirement (or fit the current knowledge). As informed by research in the ergonomics arena, the bridge's serviceability regarding the users' feelings is increasingly discussed based on the vibration experienced by the users (i.e., human body vibration). For bridge VIV in particular, a number of studies have been conducted as prompted by the frequent VIV occurrences of LSBs in recent years. For instance, Yu et al. [16] examined the effect of bridges' VIVs on the ride comfort of a single vehicle crossing the bridge, revealing that VIVs could aggravate the dynamic vehicle responses and thereby cause more severe discomfort issues. Zhu et al. [11] assessed the drivers' ride comfort when traveling on a long-span suspension bridge under VIVs in the context of the wind-traffic-bridge system based on the criteria recommended in ISO 2631-1. They disclosed that the dynamic interaction between the stochastic traffic flow and the bridge can also affect the driver's ride comfort apart from the bridge's VIV, and traffic density and proportion can affect this interaction and the resulting ride comfort. More recently, Zhang et al. [17] considered the multimode lock-in characteristics of the VIV of LSBs and studied the dynamic behavior and ride comfort of a single vehicle running on the bridge.

In general, the aforementioned studies focused more on developing methods to realistically simulate the human body vibration of the bridge users under a bridge VIV event, leading to a consensus that a realistic reproduction of real-world wind-traffic-bridge system is quite essential to understand the associated human body vibration of the bridge users and thus their feelings. However, most studies only provided vibration simulation methods for the users inside vehicles crossing the bridge but ignored the pedestrians standing on the bridge. More importantly, the ultimate human body vibration (or feelings) assessment was not considered seriously but simply followed a popular routine (i.e., using the overall vibration total value (OVTV) recommended in ISO 2631-1 [18] to identify the unpleasant feelings of the users of a bridge under VIVs). Actually, engineering practice has revealed that the frequencies (f) of VIVs occurring on most LSBs are very low (e.g., $f \leq 0.5$ Hz). Rather, the currently popular OVTV was designed for characterizing human's discomfort that is sensitive to vibration in the frequency range of 0.5~80 Hz, which makes its

ability to distinguish unpleasant users' feelings originating from the bridge's VIVs questionable. In view of this, this study attempts to revisit the serviceability of LSBs under VIVs in terms of human's motion sickness that has been found to be triggered by vibration below 0.5 Hz. Additionally, a comprehensive examination of the influence of VIV and traffic flow on the bridge serviceability (users' feelings) is performed both from the perspective of vehicle riders and pedestrians.

The remainder of this paper is organized as follows. Section 2 introduces the general computational framework of bridge users' human body vibration and the associated feeling assessment method. In Section 3, the serviceability of LSBs under VIVs is studied with a single vehicle crossing the bridge, trying to reveal the influence of VIV itself. In Section 4, the serviceability is evaluated in the context of a wind-traffic-bridge system to disclose how VIV and traffic load together affect users' feelings. Finally, Section 5 concludes the entire paper.

2. Evaluation Procedure of Human Body Vibration for Users of the Bridge under VIVs

Evaluating the bridge users' feelings on a subjected vibration based on numerical simulation requires two critical parts, which are a wind-traffic-bridge dynamic analysis framework to calculate the human body vibration of the users and a human body vibration assessment procedure to identify the users' feelings, respectively. As shown in Figure 1, the wind-traffic-bridge dynamic analysis involves the modeling of the coupled vehicle-bridge system, VIV, and traffic loading scenario, each of which contains complex details. Since these details have been well reported in the authors' previous work [11, 19], this study only provides a summarizing demonstration and accessible references of each ingredient in Section 2.1. For the human body vibration assessment procedure that has been seldom reported in the literature, the authors presented a detailed demonstration of how to obtain the index for determining users' feelings based on the objective human body vibration of a user and the specific feeling criteria in Section 2.2.

2.1. Wind-Traffic-Bridge Dynamic Analysis for the Bridge under VIVs. The general computational framework of the wind-traffic-bridge system with a bridge experiencing VIVs includes two major ingredients: the VIV modeling and vibration analysis shown in Figure 1. Specifically, the vortex-induced force (VIF) model is adopted to replicate the VIV of the bridge. Since the main focus of this study is to build a general evaluation framework and to examine the effect of VIV on bridge users' feelings, the harmonic VIF model [20] that exclusively depicts the force caused by the shedding of vortices from the bluff body (i.e., the major excitation of VIVs) is considered for easy implementation, which can be expressed as

$$F_{VI} = \frac{1}{2} \rho U^2 D \tilde{C}_L \sin(\omega t + \theta), \quad (1)$$

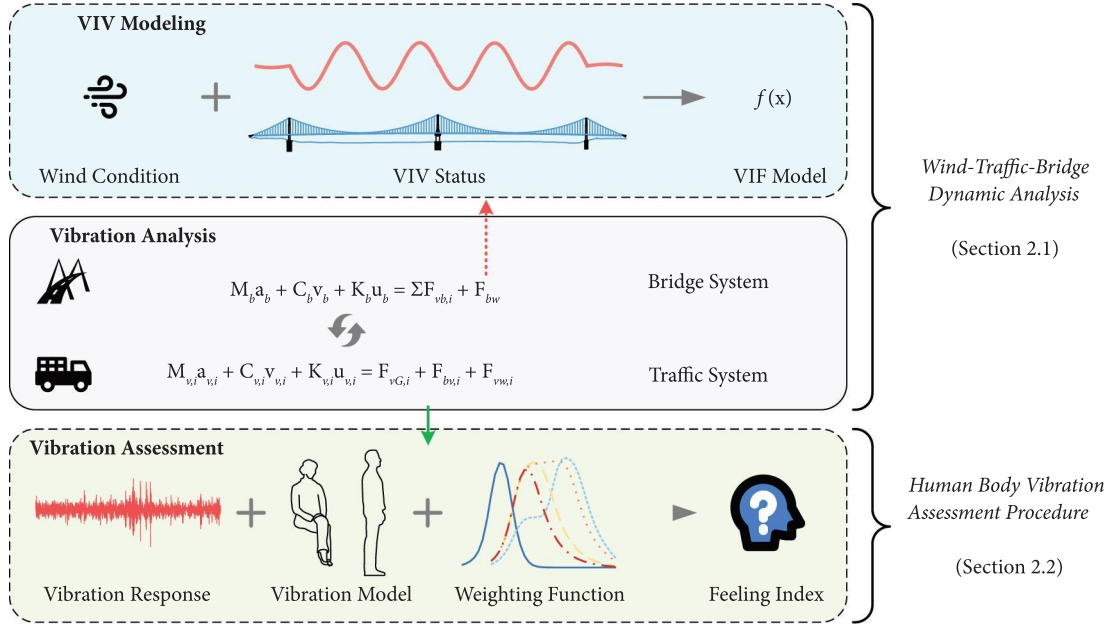


FIGURE 1: Evaluation procedure of human body vibration for users of the bridge under VIVs.

in which ρ represents the air density; U denotes the wind speed; D is the deck depth; \bar{C}_L is the root-mean-square (RMS) value of the lift aerodynamic force coefficient; ω is the circular frequency of the vortex shedding, which can be obtained as $\omega = 2\pi f_b$ (f_b is the VIV frequency); t denotes time in seconds; and θ is the phase difference between VIF and VIV. The determination of the VIF model parameters often requires massive wind tunnel tests, which can be time-consuming and cost-prohibitive. Alternatively, an inverse identification method of the VIF model parameters based on dynamic analysis is recommended. The idea is to compare the VIV amplitude caused by unit VIF (calculated by dynamic analysis) and the VIV amplitude of interest. Previous studies of the authors have demonstrated that the adopted VIF model and model parameter identification method have a good performance in simulating VIVs of LSBs according to field monitoring data, and readers may refer to Zhu et al. [11] for more details. Note that, in the present study, the VIF model parameters will be calculated in terms of the condition that the LSB only suffers from the VIF, and several groups of parameters will be discussed to investigate the effect of VIV severities (i.e., the VIV amplitude) on human body vibration and users' feelings. Once the VIF model parameters are obtained, the VIF can be conveniently included in the subsequent coupled vibration analysis. Therein, the aerodynamic behavior of the bridge is simulated solely by the VIF, and the wind effect on the vehicle is reproduced based on the corresponding turbulent wind field.

With explicit excitations from the wind, the governing equations of the wind-traffic-bridge system can be expressed as follows:

$$M_b \mathbf{a}_b + C_b \mathbf{v}_b + K_b \mathbf{u}_b = \sum_{i=1}^n \mathbf{F}_{vb,i} + \mathbf{F}_{bw}, \quad (2)$$

$$M_{v,i} \mathbf{a}_{v,i} + C_{v,i} \mathbf{v}_{v,i} + K_{v,i} \mathbf{u}_{v,i} = \mathbf{F}_{vG,i} + \mathbf{F}_{bv,i} + \mathbf{F}_{vw,i}, \quad (3)$$

where i denotes the i th vehicle on the bridge (n is the total vehicle amount); the subscripts b and v denote the bridge and vehicle; M , C , and K are the mass, damping, and stiffness matrices, obtained from finite element modeling for the bridge or multibody dynamics simulation for the vehicle; and \mathbf{a} , \mathbf{v} , and \mathbf{u} are the acceleration, velocity, and displacement vectors. The force term $\mathbf{F}_{vG,i}$ represents the weight of the i th vehicle. $\mathbf{F}_{bv,i}$ and $\mathbf{F}_{vb,i}$ are the coupled vehicle-bridge forces (i.e., interactions) at the contact points between i th vehicle and the bridge, which are related to the bridge and vehicle vibration status and the road roughness excitation [21]. The aerodynamic behavior of the bridge is determined by an elementwise force vector acting on the bridge girder as follows:

$$\mathbf{F}_{bw} = \int_0^L \varphi_n(x) \cdot F_{V1}(t) dx, \quad (4)$$

where $\varphi_n(x)$ denotes the n th VIV mode shape of the bridge and L is the bridge span length. By applying specific \mathbf{F}_{bw} to the bridge's model, different modes of VIV can be reflected. As for the vehicle, the quasistatic aerodynamic forces are adopted to describe the associated wind effect (\mathbf{F}_{vw}) according to [22]. In this way, the complex interactions between wind, traffic (or vehicles), and the bridge can be rationally modeled. Equations (2) and (3) will be solved independently through the Newmark- β method based on the force and displacement equilibriums at the vehicle-bridge contact points to obtain the ultimate system vibration.

Notably, the realistic traffic loading scenario is simulated by introducing an improved cellular automaton (CA) traffic model. CA traffic model can facilitate a spatiotemporal microscopic traffic simulation, assuming that time and space are discrete. By regulating the driving behavior (e.g., acceleration, deceleration, and lane change) of each vehicle in

the traffic flow and parallelly updating each vehicle's velocity and position, the real-world traffic phenomena can be realistically reproduced [23]. More detailed explanations can be found in the authors' previous work [19], which are omitted herein for a succinct purpose. Besides, other excitations of the system include road roughness and turbulent wind, each of which can be assumed as a stationary Gaussian stochastic process and simulated in a pretty mature way [24].

2.2. Human Body Vibration Assessment Procedure. Based on the vibration analysis, the dynamic responses of the bridge and vehicles can be obtained. As shown in Figure 1, the dynamic responses need to be further transformed for vibration assessment because the human is experiencing a compound vibration transmitted from the relevant supporting surfaces (i.e., whole-body vibration). In this case, the overall vibration measure needs to be calculated based on the vibration model of bridge users (Figure 2). Unlike the previous research focusing on the feelings of vehicle riders only, this study introduces a seated person and a standing person for the vibration (or feeling) assessment for vehicle riders and pedestrians, respectively. A seated person can experience motions from three supporting surfaces, i.e., the floor, seat, and backrest, and a standing person can only perceive the motion from the supporting floor [18].

With the whole-body vibration measure, the human feeling index can be examined with a typical routine as recommended in ISO 2631-1 [18]. For the previously popular human comfort index based on OVTV [11, 17, 25], the routine is to first get the whole-body vibration measure from vehicle/bridge responses according to the relative position between the person and the vehicle/bridge node (as the responses are calculated for discrete points). Then, those human body vibrations that are related to the human comfort index need to be frequency-weighted to show the influence of vibration frequency on human comfort. Finally, the OVTV is obtained as a human comfort indicator based on the RMS values of the frequency-weighted vibrations and some multiplying factors suggesting the influence of vibrations from different directions on human comfort. It should be noted that the frequency weighting functions for the human comfort index (W_k , W_d , W_c , and W_e in Figure 3) have relatively small values in the interested frequency range of VIVs of LSBs (e.g., below 0.5 Hz). As a result, the human body vibration originating from VIV might be filtered out in calculating OVTVs, and the influence of VIV on bridge users' feelings can be misunderstood if using human comfort (or OVTV) as an indicator.

Alternatively, this study advocates using the motion sickness index (MSI) to describe the users' feelings on VIVs of LSBs. As documented in ISO 2631-1 [18], the MSI is concerned with vibration with frequency contents below 0.5 Hz. Motion sickness generally happens when the movement that a person sees is different from what his/her inner ear senses, resulting in dizziness, nausea, and vomiting. Similar to the procedure of obtaining the human comfort index (OVTV), the calculation of MSI starts with transforming bridge/vehicle responses to the whole-body

vibration measures based on the relative position. The major influencing vibration on the MSI includes vertical, pitching, and rolling accelerations, so the vertical accelerations from three supporting faces (a_{zf} , a_{zs} , and a_{zb}) and pitching (a_{ry}) and rolling (a_{rx}) accelerations are obtained as follows:

$$\begin{aligned} a_{zf} &= a_{zs} \\ &= a_{zb} \end{aligned} \quad (5)$$

$$\begin{aligned} &= \ddot{Z}_v, \\ a_{ry} &= \ddot{\theta}_v \cdot d_s, \end{aligned} \quad (6)$$

$$a_{rx} = \ddot{\phi}_v \cdot y_s + \frac{1}{2} \ddot{\phi}_v \cdot h_s, \quad (7)$$

in which \ddot{Z}_v , $\ddot{\theta}_v$, and $\ddot{\phi}_v$ represent vertical, pitching, and rolling accelerations at the vehicle centroid and d_s , y_s , and h_s are longitudinal, transverse, and vertical distances between the vehicle centroid and the vehicle rider's seat. As for the standing person, only the vertical vibration transmitted from the floor (a_{zf}) is involved in the MSI calculation, and it is obtained as the vertical bridge acceleration at the standing point. Subsequently, the decisive accelerations for MSI are frequency-weighted based on a fast Fourier transform (FFT) convolution. In detail, the original time-history acceleration $x(k)$ (with N discrete time steps) is transformed into the frequency domain as $X(r)$ using the discrete Fourier transform (DFT):

$$X(r) = \sum_{k=0}^{N-1} x(k) \omega_N^{rk}, \quad (8)$$

where $\omega_N = e^{-2\pi r/N}$, $r=0, 1, \dots, N-1$. The frequency-domain acceleration will be weighted as $a_{wi}(t)$ (i denotes different acceleration components, e.g., subscripts zf and ry in equations (5) and (6)) according to the frequency weighting function for MSI (W_f in Figure 3). Then, the frequency-weighted acceleration is used to calculate the motion sickness dose value (MSDV) according to

$$\text{MSDV}_i = \left\{ \int_0^T [a_{wi}(t)]^2 dt \right\}^{1/2}, \quad (9)$$

in which T is the duration of the time-history acceleration in seconds. The total MSDV (MSDV_T) is obtained by adding MSDVs of all decisive accelerations for MSI (i.e., 5 acceleration components for a seated person and 1 acceleration component for a standing person), as the decisive accelerations are deemed as equally important to MSI. Finally, the MSI is calculated as follows [18]:

$$\text{MSI}(\%) = K_m \cdot \text{MSDV}_T, \quad (10)$$

where K_m is a constant related to the characteristics of persons of interest, and it is adopted as 1/3 herein for typical bridge users, mainly consisting of adults. A larger MSI value suggests that more bridge users may suffer from motion sickness and have unpleasant feelings on the VIV. It should

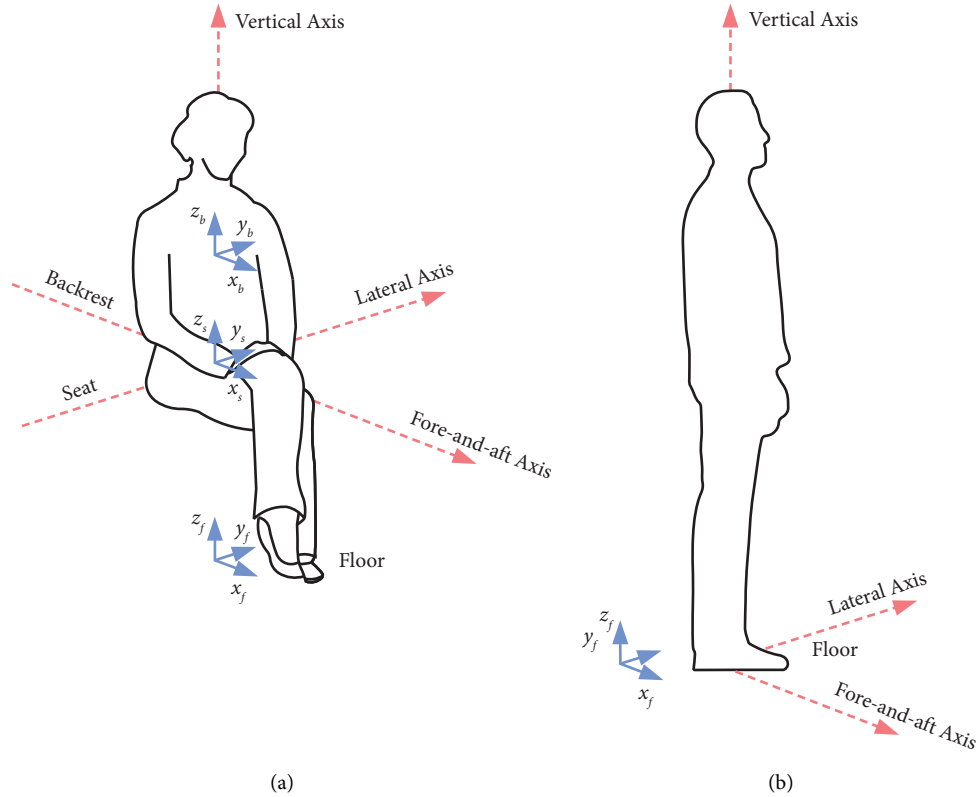


FIGURE 2: Vibration model for bridge users: (a) seated person model for vehicle riders; (b) standing person model for pedestrians.

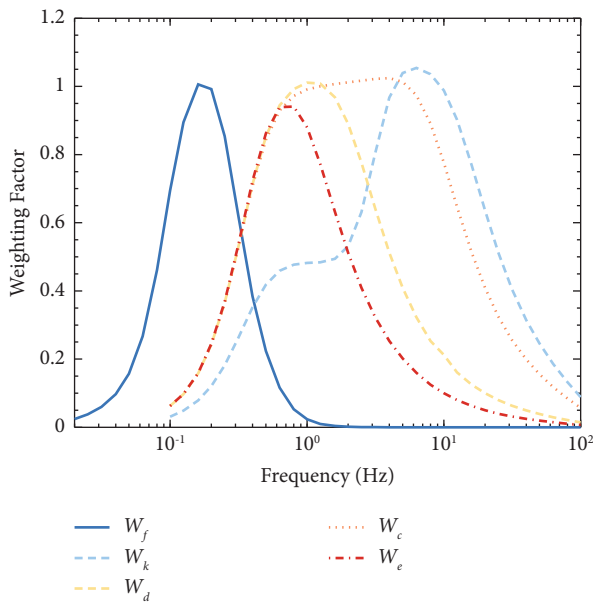


FIGURE 3: Frequency weighting functions for human body vibration assessment.

be noted that many existing studies developed motion sickness criteria in terms of structural vibration for the users of a particular structure (e.g., the occupants of wind-excited tall buildings in [26]). However, the associated outcomes can hardly be used in the present study, given the significantly

different systems being studied. By focusing on the fundamental human body vibration, the adopted MSI from a reputable standard provides a reliable measure to characterize the motion sickness of the users of a bridge experiencing VIV, which is deemed suitable for the current research focus.

3. Vibration Characteristics and Feelings of Users of the Bridge under VIV and a Single Vehicle

Currently, very few endeavors have been made to understand the influence of LSBs' VIVs on the vibration characteristics of the bridge users in the context of a wind-vehicle-bridge system, and the associated users' feelings did not receive deserved attention. In this regard, this section presents evaluations in the wind-vehicle-bridge system, where the bridge is experiencing VIVs and supports a single running vehicle. Accordingly, it can be deemed that the vibration of the seated person in the vehicle is primarily affected by the bridge's VIV and vehicle-bridge interaction, while the vibration of a standing person on the bridge is exclusively influenced by the VIV, given that a single running vehicle can cause trivial influence on the bridge vibration.

3.1. Prototype Bridge. The Yingwuzhou Yangtze River Bridge (YWB), a three-tower four-span suspension bridge, is adopted as the prototype bridge in this study. It has a total

length of 2100 m, with a span arrangement of 200 m + 2 × 850 m + 200 m (Figure 4(a)). As shown in Figure 4(b), the π -shaped steel-concrete composite stiffening girder is used, with a cross section that is 38 m in width and 3 m in height. Besides, the YWB supports two-way (with four lanes in each way) highway traffic.

As stated previously, the proposed method requires a finite element model of the bridge. To capture the overall dynamic characteristics and maintain acceptable computational efforts, the bridge's girder and pylon are idealized as 3D beam elements; the cable and suspender are simulated with 3D link elements; the stiffness contribution owing to the pavement and railing is neglected, and their masses are equally distributed to the girder using the mass-only element. Consequently, a finite element model (FEM) with 1548 nodes and 2236 elements is obtained. According to the real measurement reported in [11], the prototype bridge had a VIV event at the frequency of 0.244 Hz, which corresponds to the fourth vertical asymmetric mode ($f=0.242$ Hz) obtained in the current finite element analysis. Considering that VIVs of LSBs are likely to be excited in multiple low-order modes [17], a qualitative study of the influence of VIV modes on the vibration characteristics and users' feelings will be performed based on several vertical asymmetric modes (including $f=0.242$ Hz) as listed in Table 1. Notably, although torsional VIV modes with appreciable amplitudes can also cause unpleasant feelings in users, such VIVs are uncommon for real-world LSBs that have been carefully designed to avoid detrimental torsional vibrations and are, therefore, neglected in the present study.

3.2. Vibration Characteristics of the Bridge User. As mentioned above, only a single vehicle is considered in this section, which is selected as the most common type of vehicle traveling on the bridge, i.e., a sedan car running at 40 km/h. The sedan car is modeled as a combination of several rigid bodies and wheel axles connected by springs and dampers, which has been reported in [11] and is omitted herein.

3.2.1. Time-History Dynamic Response. The previously observed VIV ($f=0.242$ Hz) with an amplitude of 0.5 m [11] is first studied. To clarify the influence of vehicle-bridge interaction (VBI), VIV, and road roughness on the human body vibration of bridge users, three scenarios are studied with and without considering road roughness: (1) vehicle travels on the road (condition 1); (2) vehicle travels on the bridge without VIVs (condition 2); and (3) vehicle travels on the bridge under VIVs (condition 3). For those scenarios with road roughness, a very good road roughness is considered according to ISO [27]. Figures 5 and 6 depict the time-history dynamic responses of the vehicle (measured from the vehicle centroid) and bridge (measured from the vehicle-bridge (V-B) contact point) under given conditions.

As shown in Figure 5, when road roughness is neglected, there is no vibration for the vehicle traveling on the road, and the VBI in condition 2 causes trivial vehicle vibration (i.e., a maximum vertical acceleration (MVA) of 0.0339 m/

s^2). However, the VIV and VBI can cause significant vertical vehicle vibration in condition 3 (namely, a MVA of 1.3798 m/s^2), and the VIV is the primary excitation because the MVA at the V-B contact point is 1.1506 m/s^2 . The difference between the time-history accelerations of the vehicle centroid and the V-B contact point suggests that the perceived vibration for vehicle riders and pedestrians can be different, but generally, the bridge vibration is a baseline for the vehicle vibration because of the displacement equilibrium.

When road roughness is considered (Figure 6), the vehicle vibration becomes more significant, and the MVAs at the vehicle centroid for condition 1 and 2 become 1.4135 and 1.4253 m/s^2 , respectively. In condition 3, the MVA at the vehicle centroid increases to 2.1331 m/s^2 . But for the vertical acceleration at the V-B contact point, the MVA just increases slightly after considering road roughness, which can be because the VBI caused by a single vehicle (even if it is aggregated by road roughness) has a trivial influence on the vibration of LSBs.

Generally, it can be concluded that the bridge vibration is closely related to the VIV and VBI, which can further affect the vibration of the running vehicle on the bridge. Although the bridge vibration serves as a baseline of the vehicle vibration, the vehicle vibration is typically more significant than the bridge vibration at the V-B contact point. Hence, for vehicle riders and pedestrians, the associated feelings on the bridge expiring VIVs might be different. Moreover, road roughness can aggregate the vehicle and bridge vibration, but its influence on users' feelings remains unclear.

3.2.2. Power Spectrum Density. The bridge users' feelings on a vibration are highly dependent on the frequency of the vibration. This section further examines the power spectrum density (PSD) of the vertical acceleration at the vehicle centroid for conditions 2 and 3 introduced in Section 3.2.1. Figure 7 describes the PSD features under no road roughness condition, in which the vehicle vibration in condition 2 exclusively originates from the VBI, and the vehicle vibration in condition 3 is caused by the VIV and VBI. It can be seen from Figure 7(a) that the VBI primarily excites the vehicle vibration in relatively high frequencies (e.g., above 3 Hz). The two obvious peaks in Figure 7(a) are at frequencies of 2.968 and 3.7 Hz, which are close to the frequencies of two high-order vertical bridge modes (i.e., 2.971 and 3.705 Hz). However, for condition 3 in Figure 7(b), the major frequency contents of vehicle vibration are near the frequency of VIV (0.242 Hz). Notably, there are two peaks enclosing the VIV frequency, which can be attributed to the Doppler effect [28] caused by the vehicle moving in a coupling vehicle-bridge system. This phenomenon can ultimately make the feelings of bridge users on moving vehicles unique because the contribution of the bridge's VIVs becomes two major components acting on the human body, each of which may have a different significance on the feeling depending on the associated frequency.

When considering road roughness (Figure 8), the PSD of vehicle acceleration becomes more chaotic, but it can be seen that most vibration energy concentrates in the range that is

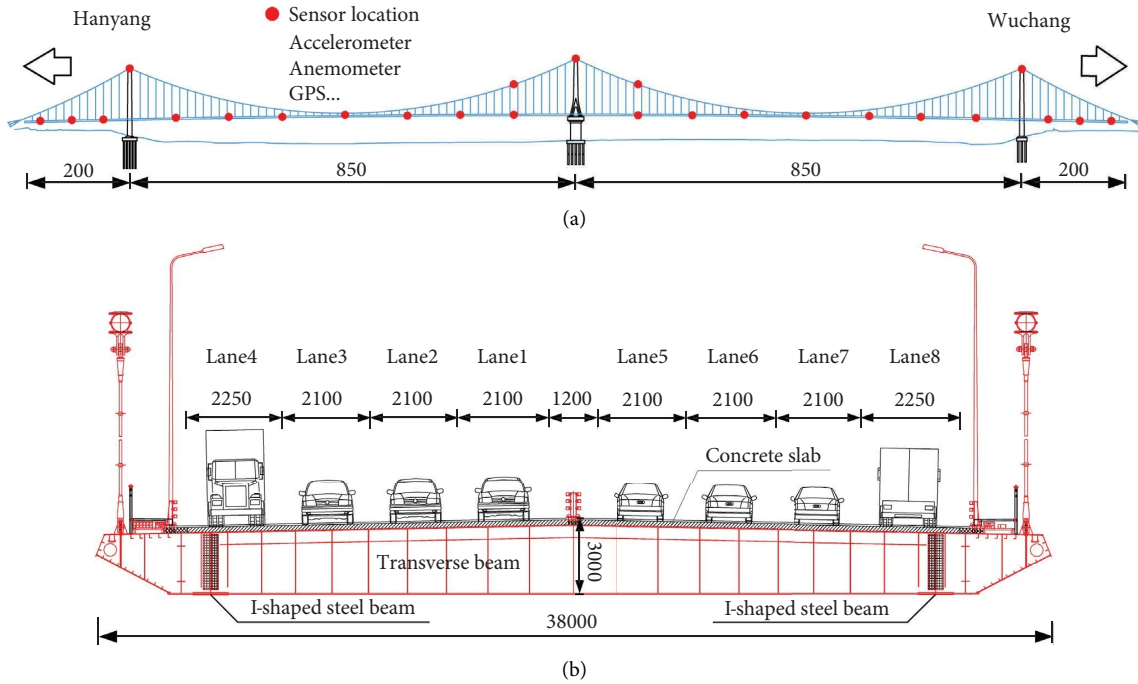


FIGURE 4: Yingwuzhou Yangtze River Bridge: (a) elevation view of the entire bridge (m); (b) cross section of the main girder (mm).

TABLE 1: Typical low-order vertical asymmetric modes of YWB.

Frequency (Hz)	Mode shape description
0.101	
0.128	
0.242	
0.378	
0.531	

near the most obvious peaks in Figure 7 (e.g., 2–5 Hz for condition 2 and 0.2–0.3 Hz for condition 3). In particular, as shown in Figure 8(b), even if the VIV is the major excitation in this condition, the influence of road roughness can be observed in the frequency range of around 3–4 Hz. Therefore, it can be found that the vehicle vibration characteristics are closely related to the bridge vibration, which is dominated by the VIV and VBI in our context. The VIV mainly causes vehicle vibration in a low frequency range (typically below 0.5 Hz), and the VBI can excite the vehicle vibration in a relatively high frequency range (e.g., above 3 Hz). Road

roughness can make the vehicle vibration more chaotic, but the dominant frequency range remains the one originating from the V-B coupled vibration.

3.3. Bridge Users' Feelings. The vibration characteristic analysis helps to understand the influencing mechanisms of VIV, VBI, and road roughness on users' human body vibration. On this basis, this section further examines users' feelings, following the same case setting in Section 3.2. Specifically, the users' feelings are assessed for the driver of the sedan car running at 40 km/h and a pedestrian standing on the 3/8 span of the first main span of YWB (i.e., one crest of this VIV ($f=0.242$ Hz), which can lead to the maximum human body vibration for standing persons). Since the MSI is correlated to the time duration of the vibration (see (9)), the users' feelings are evaluated based on the entire process ($T=2100/(40/3.6)=189$ s) of the vehicle crossing the bridge both for the driver and pedestrian for a fair comparison.

3.3.1. Comparison of Human Comfort Index and Motion Sickness Index. As mentioned previously, the currently popular index for human body vibration (or users' feelings) assessment might be unsuitable to investigate the effect of VIV because of the low-frequency characteristics of LSBs' VIVs. In specific, the VIVs can cause excitations on the bridge users' bodies primarily in a range with low frequencies (e.g., below 0.5 Hz) rather than in a conventional range that is within the scope of OVTV including the resonance frequency of the human body (e.g., 4–7 Hz). Hence, this section presents a very important discussion by comparing the human comfort index and motion sickness

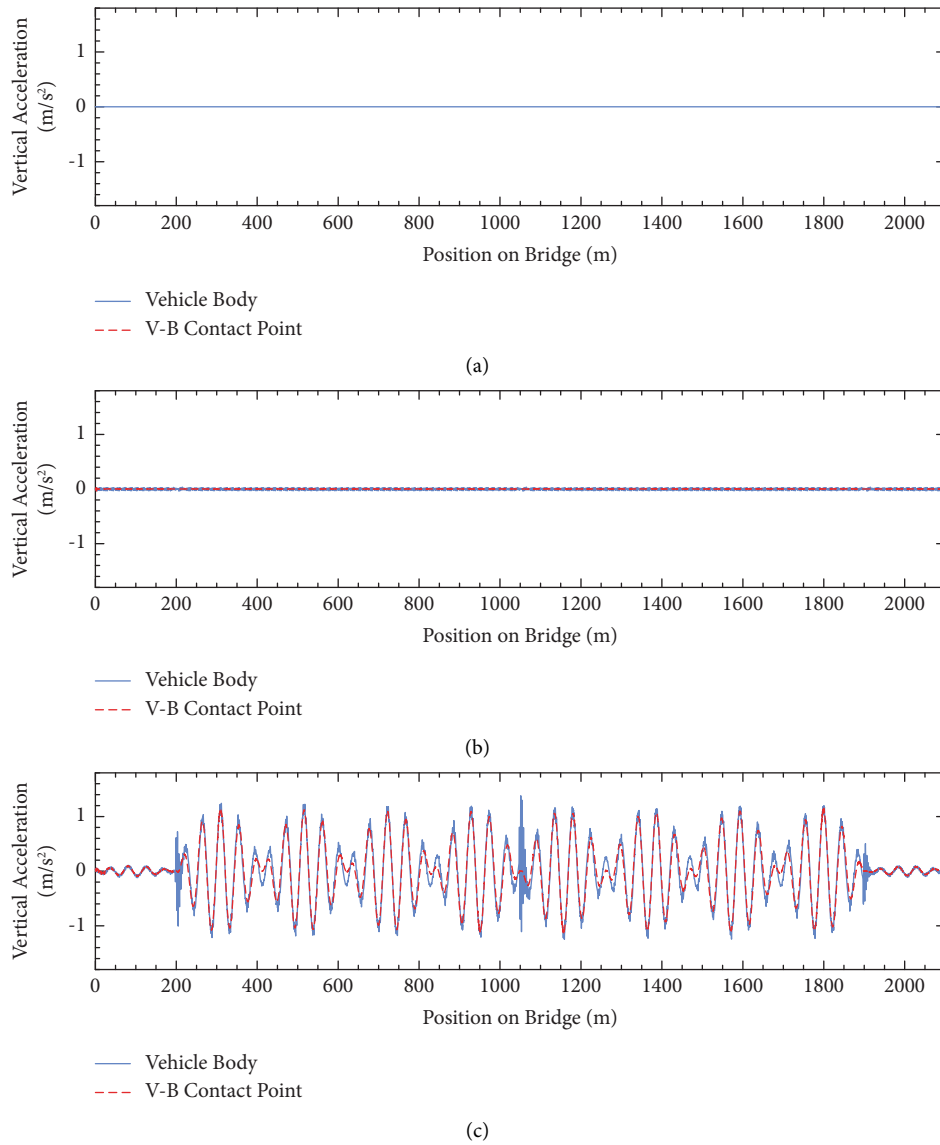


FIGURE 5: Vertical accelerations at the vehicle centroid and the vehicle-bridge contact point under given conditions without road roughness: (a) condition 1; (b) condition 2; (c) condition 3.

index based on conditions 1, 2, and 3 described before, and an additional road roughness condition (average road roughness) is considered. The calculation procedure of MSI follows the one presented in this study, and that of the human comfort index (i.e., OVTV) can be found in the previous work [11, 17]. The MSI and OVTV for different conditions are summarized in Table 2.

Interestingly, it is found that the OVTV is indeed an inappropriate index for studying the influence of VIVs on bridge users' feelings, especially in terms of vehicle riders. As listed in Table 2, the OVTV for the vehicle driver in the very good road roughness condition only increases from 0.3846 m/s^2 to 0.4185 m/s^2 after considering VIV. Different from the trivial influence of VIVs on the OVTV, road roughness can affect the OVTV significantly. For the vehicle driver in condition 3, the OVTV increases obviously from 0.4185 m/s^2 to 1.1068 m/s^2 as road roughness gets worse.

Nevertheless, the MSI appears to be a pretty good index to characterize the influence of VIVs on bridge users' feelings. As shown in Table 2, after considering the VIV, the MSIs of the vehicle driver and pedestrian increase significantly, and the MSI is nearly free from the influence of road roughness. For the example with a very good road roughness condition, the MSI of the vehicle driver increases from 0.02% to 3.49% after considering VIVs, but the MSI remains 3.49% as the road roughness condition becomes average. Similar patterns can be found in the MSI of the pedestrian, but it can be seen that the MSI of the pedestrian is lower than that of the vehicle driver.

Therefore, it can be clarified that using the OVTV (human comfort index) is suitable to distinguish the effect of road roughness on bridge users' feelings, while the potential serviceability issue caused by VIVs of LSBs might be neglected. In other words, as long as road roughness remains

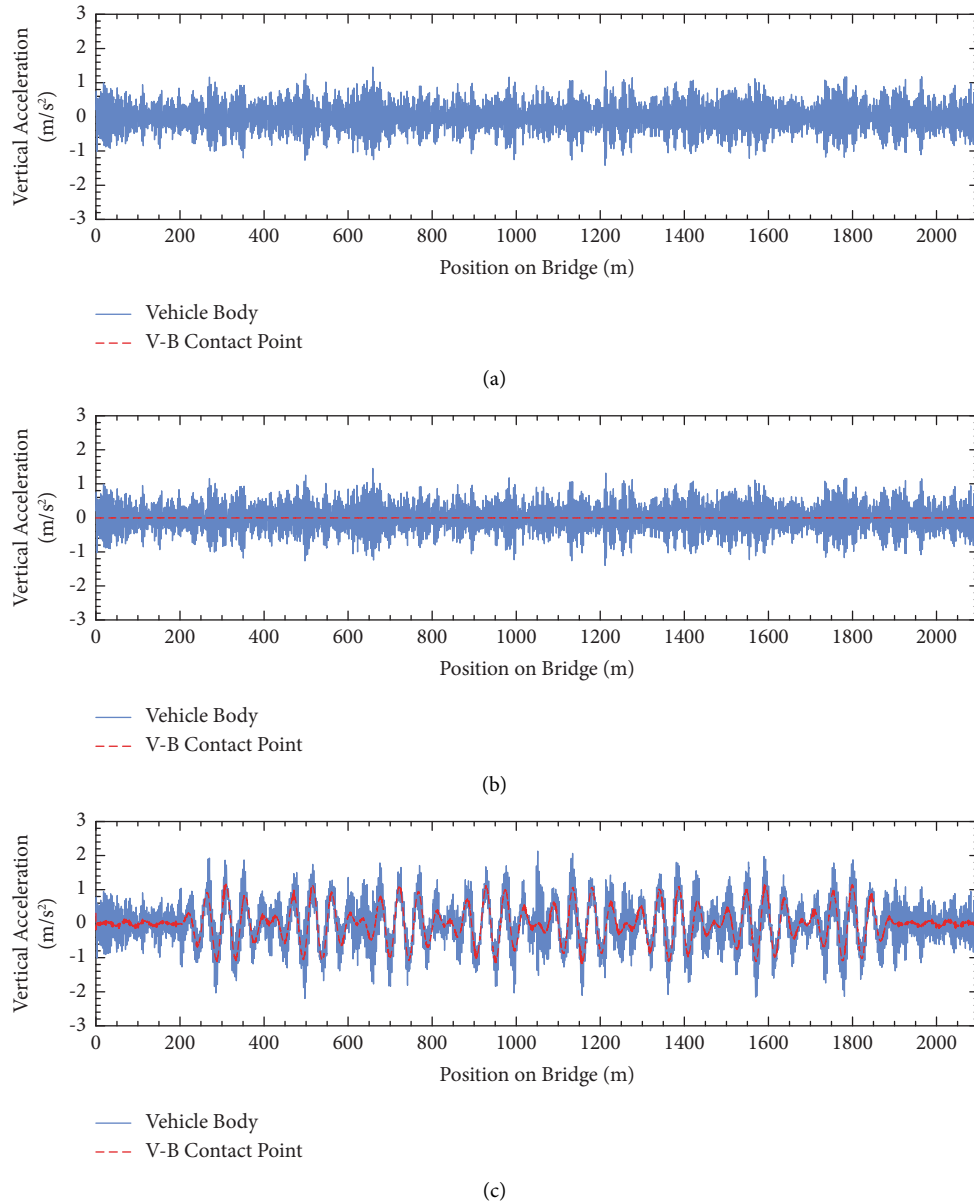


FIGURE 6: Vertical accelerations at the vehicle centroid and the vehicle-bridge contact point under given conditions with road roughness: (a) condition 1; (b) condition 2; (c) condition 3.

the same, one may always obtain similar OVTVs under different VIV events. This issue can also be found in a recent study discussing the effect of the multimode lock-in property of VIVs on vehicle riders' OVTVs [17]. In that study, different VIV modes only cause trivial differences in OVTVs (e.g., in 10^{-2} -level), but a worse level of road roughness easily leads to a significantly larger OVTV (e.g., in 10^0 -level). Rather, using the MSI can obviously identify the serviceability issue for LSBs under VIVs in terms of users' feelings, i.e., the unpleasant feeling of the users of the bridge under VIVs can be distinctly predicted from the calculated MSI.

3.3.2. Influence of Vehicle Speed, VIV Amplitude, and VIV Frequency. Having disclosed that the MSI is a proper index to identify people's unpleasant feelings on VIVs, the

serviceability issue of LSBs under VIVs is discussed using the MSI hereafter. In this section, the influence of vehicle speed, VIV amplitude, and VIV frequency (or mode) is studied. Similarly, only a single sedan car crossing YWB at 40 km/h is considered. Since previous studies have implied that the MSI is nearly free from the influence of road roughness, it is assumed that the bridge is smooth.

The influence of vehicle speed and VIV amplitude on the MSI is investigated based on the previously adopted VIV with $f=0.242$ Hz. As shown in Figures 9(a) and 9(b), the MSIs for the vehicle driver and pedestrian are similar under various conditions, but the vehicle driver often has larger MSIs. It is intuitive that a larger VIV amplitude can lead to a larger MSI, and a vehicle with a lower speed can have a larger MSI because of the longer time duration of staying

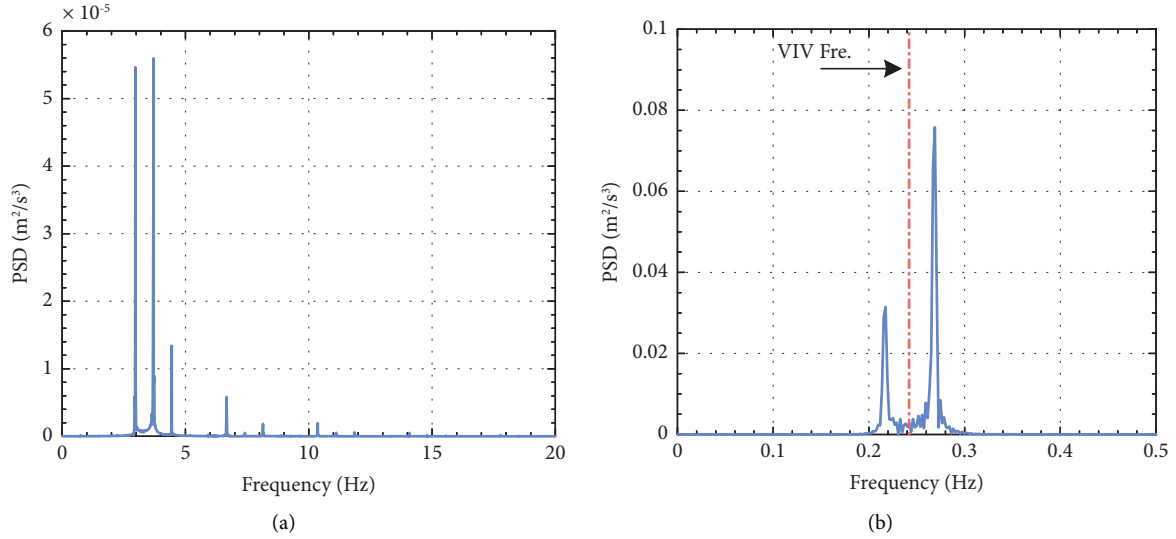


FIGURE 7: PSDs of the vertical acceleration at the vehicle centroid without road roughness: (a) condition 2; (b) condition 3.

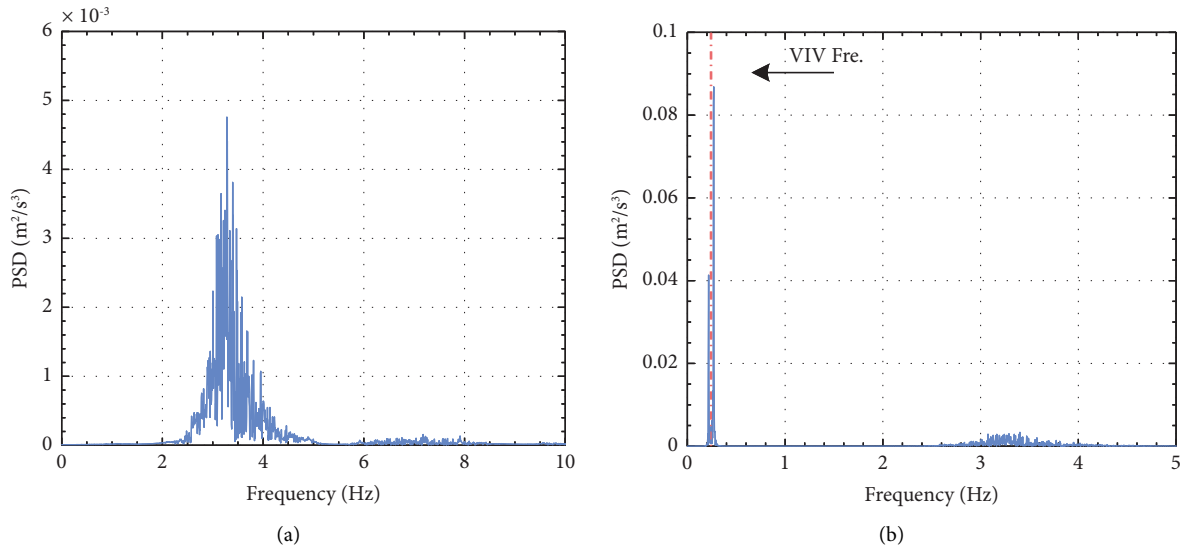


FIGURE 8: PSDs of the vertical acceleration at the vehicle centroid with road roughness: (a) condition 2; (b) condition 3.

TABLE 2: Feeling indexes of users of the bridge under VIV and a single vehicle.

Index	Condition	Vehicle driver			Pedestrian		
		No	Very good	Average	No	Very good	Average
OVTV (m/s^2)	1	0	0.3840	1.0861	—	—	—
	2	0.0149	0.3846	1.0872	$1.62E-04$	$2.27E-04$	$4.74E-04$
	3	0.1478	0.4185	1.1068	0.1363	0.1363	0.1364
MSI (%)	1	0	0.02	0.05	—	—	—
	2	$1.06E-03$	0.02	0.05	$5.20E-04$	$5.47E-04$	$6.03E-04$
	3	3.49	3.49	3.49	3.18	3.18	3.18

on (or for crossing) the bridge experiencing VIVs. The effect of VIV frequency and amplitude is exclusively studied on the sedan car running at 40 km/h, addressing all VIV modes listed in Table 1. It can be seen from Figures 9(c) and 9(d)

that the MSI of bridge users first increases with VIV frequency but will finally decrease as the VIV frequency is beyond a specific value. For instance, when adopting the VIV amplitude as 0.5 m, the MSIs of the vehicle driver are

0.4406%, 0.9797%, 3.4915%, 4.5115%, and 4.0365% for the VIVs at the frequency of 0.101, 0.128, 0.242, 0.378, and 0.531 Hz.

The results can be attributed to the following two reasons. Firstly, as shown in Figure 3, W_f increases with the frequency in the range of 0–0.166 Hz and then decreases until $f=0.5$ Hz, indicating an inverting decrease in MSI results starting at 0.387 Hz for the adopted VIV frequencies is not surprising. Secondly, although the maximum W_f is obtained at $f=0.166$ Hz, the higher energy contained in a relatively high-frequency VIV leads to a maximum MSI at $f=0.378$ Hz, given the same vibration amplitude for all frequencies under investigation.

4. Users' Feelings for the Bridge under VIV and Traffic

In addition to the single-vehicle loading scenario in Section 3, users' feelings for the bridge under VIV and realistic traffic are often of more interest for understanding the real-world serviceability issue. Hence, the stochastic traffic flow is incorporated, following the authors' recent work [11, 19]. In specific, a 2500 m-long road-bridge-road system is utilized to simulate random traffic flows based on the improved CA traffic model in [19]. Herein, a road-bridge-road system can ensure the vehicle entering the bridge in a vibrating status as caused by road excitations to reproduce real-world phenomena and can help to simulate traffic behavior from a transportation network perspective [23]. Four types of vehicles, including sedan car, minivan, motor bus, and semi-trailer truck, are considered to replicate heterogeneous traffic compositions, and three typical traffic densities (12, 25, and 40 vehicles/km/lane) are studied. The traffic flow is assumed to be equally distributed on all lanes of YWB, each of which consists of 70% sedan cars, 10% minivans, 10% motor buses, and 10% semi-trailer trucks. For different vehicle types, different model structures and parameters (e.g., mass, stiffness, and damping) are adopted according to [29] to reflect the associated dynamic properties, and specific driving features (e.g., acceleration rate and deceleration rate) are included in the CA traffic model. Overall, realistic traffic phenomena, like traffic congestion and its propagation, can be reproduced from the improved CA traffic flow, resulting in a reliable traffic loading scenario. Subsequently, the system will be analyzed for 800 s in a time step of 0.04 s, which allows an adequate evolution of traffic flows to reflect various traffic distributions on the bridge and helps generate enough samples for calculating MSIs (each one refers to one sample of the feeling on crossing the entire bridge experiencing VIVs) for a statistical pursuit. Similarly, the influence of VIV frequency and VIV amplitude is discussed in terms of the values same as those in Section 3. Notably, an 800 s-long simulation can take around 20 hours on a workstation with AMD Ryzen Threadripper 3970×32-Core @ 3.69 GHz processor when involving a free traffic flow, and the computational cost increases with traffic density.

4.1. Vehicle Rider. As mentioned above, a statistical evaluation of the MSI of vehicle riders under various conditions is preferred, considering the stochastic nature of traffic flows.

Specifically, during the 800 s-long simulations, multiple vehicles can cross the entire bridge. It is, therefore, more rational to collect all MSI samples, each of which represents the feeling of a vehicle rider on crossing the entire bridge under VIVs in a unique trajectory and time duration. Herein, the MSI samples of the same vehicle type are grouped and separately studied. It is found that for the four types of vehicles under consideration, the statistical characteristics of MSIs are similar. So, the most common bridge user, i.e., the sedan car driver, is discussed in detail.

Figure 10 presents the violin plot of MSI samples of sedan car drivers under different VIV frequencies, VIV amplitudes, and traffic densities, and the corresponding mean value and coefficient of variance (CoV) are listed in Tables 3 and 4. In terms of the influence of VIV frequency and VIV amplitude, the following observations are obtained: the mean MSI for sedan car drivers consistently increases with the VIV amplitude, and the mean MSI increases gradually for VIV frequencies of 0.101, 0.128, 0.242, and 0.378 Hz but then decreases when the VIV frequency turns into 0.531 Hz from 0.378 Hz. For instance, the mean MSIs for sedan car drivers of the moderate traffic flow (i.e., with a traffic density of 25 vehicles/km/lane) on YWB experiencing VIVs at 0.378 Hz with 0.1, 0.3, 0.5, 0.7, and 0.9 m amplitudes are 0.38%, 0.97%, 1.59%, 2.21%, and 2.84%, respectively; the mean MSIs regarding VIVs with a 0.9 m amplitude at frequencies of 0.101, 0.128, 0.242, 0.378, and 0.531 Hz are 0.39%, 0.72%, 2.20%, 2.84%, and 2.83%, respectively.

More interesting findings are about the influence of traffic density. First, the traffic load is found to be able to mitigate the adverse effect of VIVs on the MSI (or the bridge serviceability). As the traffic density increases, the MSI of sedan car drivers tends to decrease, which can be seen both from the violin plot (Figure 10) and the mean MSI. For example, for VIV frequency = 0.378 Hz and VIV amplitude = 0.9 m, the mean MSIs are 3.94%, 2.84%, and 2.47% for free, moderate, and busy traffic flows (traffic density = 12, 25, and 40 vehicles/km/lane). The larger MSI (9.07%) obtained in Section 3 (i.e., only one vehicle is loaded on the bridge) for the same VIV condition also proves this phenomenon. Secondly, the trajectories/time durations of sedan cars crossing the bridge are often more irregular, resulting in larger CoVs of the MSI. For VIV frequency = 0.378 Hz and VIV amplitude = 0.9 m, the CoVs of the MSI are 0.03, 0.03, and 0.18 for free, moderate, and busy traffic flows. This is because there is heavy congestion in the busy traffic flow, and different drivers can take significantly different time durations to cross the entire bridge, leading to pretty diverse MSIs. To show this, the mean value and CoV of time durations for sedan cars crossing the bridge are calculated as 105.48 s (0.002), 105.57 s (0.004), and 167.00 s (0.417) for free, moderate, and busy flows.

4.2. Pedestrian. Finally, the MSI for pedestrians standing on the bridge is assessed. Particularly, the time duration for calculating pedestrians' MSIs is selected as the mean value of those of sedan car riders mentioned above. Considering that the time history of vibration can affect the MSI calculation,

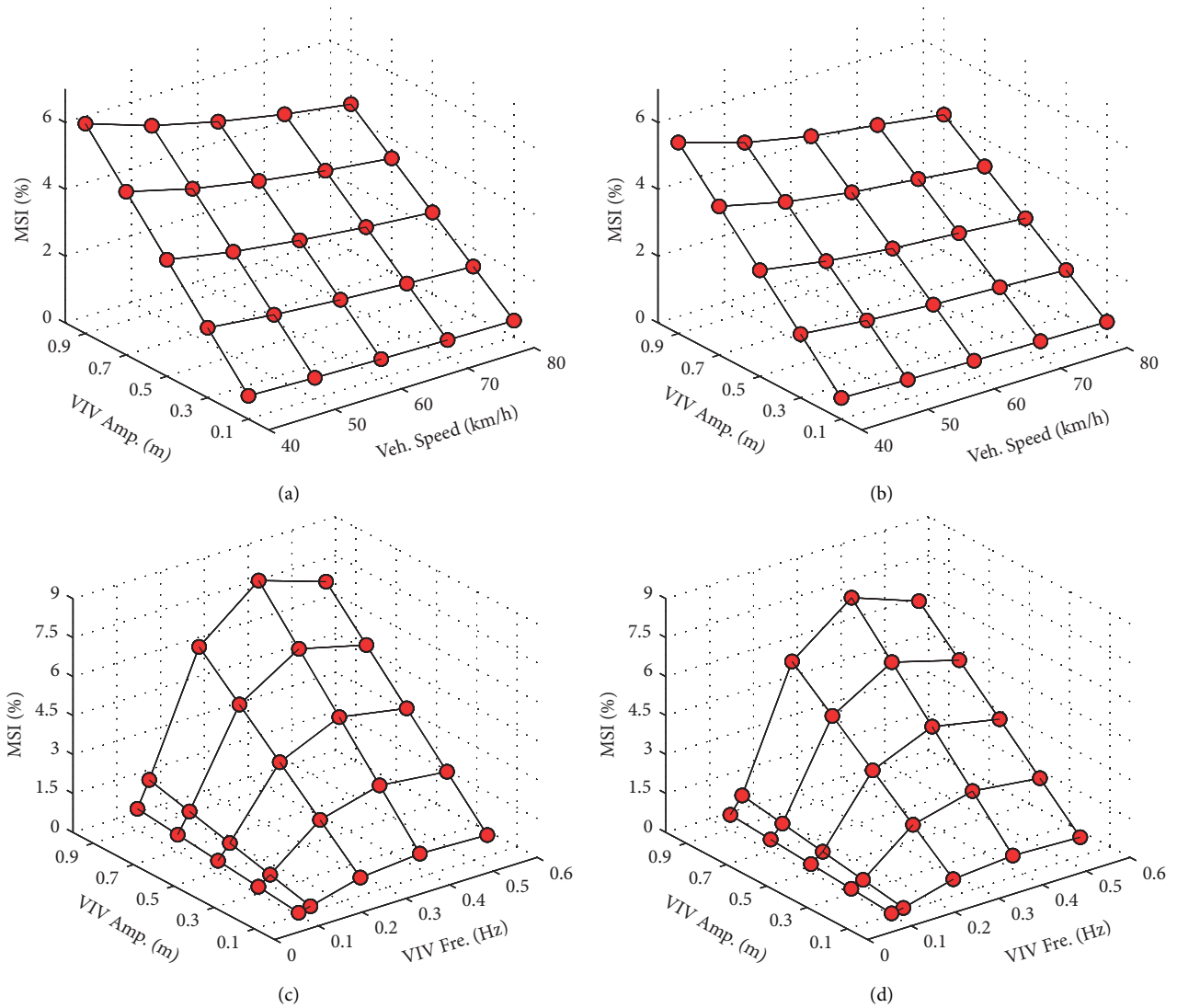


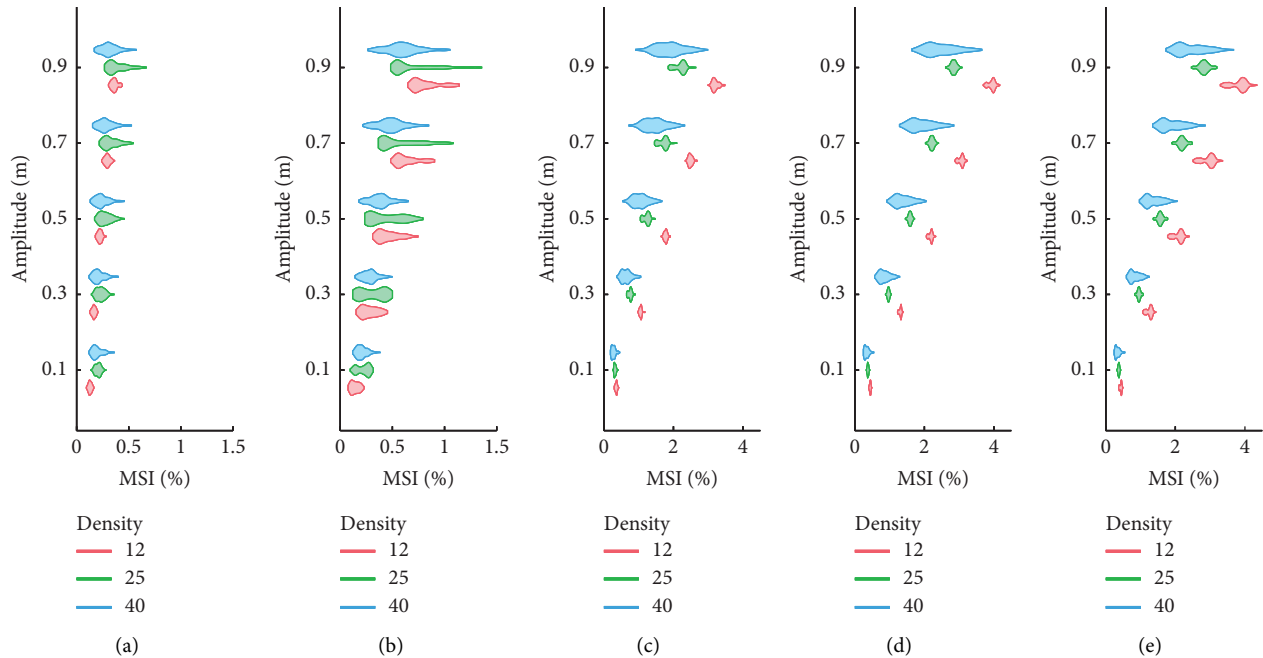
FIGURE 9: MSIs of the vehicle rider (a, c) and pedestrian (b, d) under different conditions: (a, b) different vehicle speeds and VIV amplitudes; (c, d) different VIV frequencies and amplitudes.

TABLE 3: Mean value of MSIs of sedan car drivers under different VIV frequencies, VIV amplitudes, and traffic densities (%).

VIV frequency (Hz)	Traffic density (vehicles/km/lane)	VIV amplitude (m)				
		0.1	0.3	0.5	0.7	0.9
0.101	12	0.13	0.17	0.22	0.30	0.36
	25	0.21	0.23	0.28	0.33	0.39
	40	0.20	0.22	0.24	0.28	0.32
0.128	12	0.14	0.28	0.46	0.64	0.82
	25	0.22	0.31	0.44	0.58	0.72
	40	0.21	0.28	0.38	0.48	0.60
0.242	12	0.35	1.05	1.78	2.49	3.20
	25	0.32	0.75	1.23	1.72	2.20
	40	0.28	0.65	1.06	1.47	1.89
0.378	12	0.44	1.31	2.18	3.06	3.94
	25	0.38	0.97	1.59	2.21	2.84
	40	0.34	0.85	1.39	1.93	2.47
0.531	12	0.43	1.25	2.09	2.94	3.82
	25	0.37	0.95	1.57	2.19	2.83
	40	0.34	0.84	1.37	1.91	2.46

TABLE 4: CoV of MSIs of sedan car drivers under different VIV frequencies, VIV amplitudes, and traffic densities.

VIV frequency (Hz)	Traffic density (vehicles/km/lane)	VIV amplitude (m)				
		0.1	0.3	0.5	0.7	0.9
0.101	12	0.12	0.10	0.09	0.08	0.08
	25	0.13	0.18	0.21	0.22	0.24
	40	0.24	0.26	0.26	0.27	0.26
0.128	12	0.27	0.28	0.22	0.17	0.16
	25	0.27	0.38	0.36	0.33	0.31
	40	0.24	0.25	0.26	0.26	0.26
0.242	12	0.07	0.03	0.03	0.02	0.03
	25	0.08	0.07	0.07	0.07	0.07
	40	0.20	0.22	0.21	0.21	0.21
0.378	12	0.03	0.03	0.02	0.02	0.03
	25	0.05	0.03	0.03	0.03	0.03
	40	0.18	0.18	0.18	0.18	0.18
0.531	12	0.06	0.07	0.07	0.06	0.06
	25	0.05	0.05	0.05	0.05	0.05
	40	0.19	0.18	0.18	0.18	0.18

FIGURE 10: Violin plots of MSIs of sedan car drivers under different VIV frequencies, VIV amplitudes, and traffic densities: (a) $f=0.101$ Hz; (b) $f=0.128$ Hz; (c) $f=0.242$ Hz; (d) $f=0.378$ Hz; (e) $f=0.531$ Hz.

a bootstrapping strategy is adopted to improve the reliability of the result. In specific, 10^4 records of vibration are obtained from bootstrapping: randomly extracting each record with the expected time duration from the totally 800 s-long vibration results. Then, the MSI of pedestrians is calculated as the mean value of the 10^4 records (or MSIs). Notably, the location of the pedestrian on the bridge can also influence the MSI, which is related to the mode shape of the VIV. Hence, the MSI is evaluated for several standing locations regarding VIVs of different frequencies (with a 0.9 m amplitude).

Figure 11 shows the MSIs evaluated at several typical locations of the first main span of YWB under different VIV frequencies and traffic densities. Figures 11(a) and 11(b) show the evolution of the MSI along different locations other than crests/troughs of the VIV wave, and Figures 11(c)–11(e) depict the evolution among different wave crests, nodes (zero wave amplitude), and troughs. For a better illustration, the selected locations for different VIV frequencies are explained as follows: (1) for $f=0.101$ Hz, there is only a half wave for the first (left) main span, as shown in Table 1, so the 1/2 (4/8) span location suggests a wave trough; (2) for

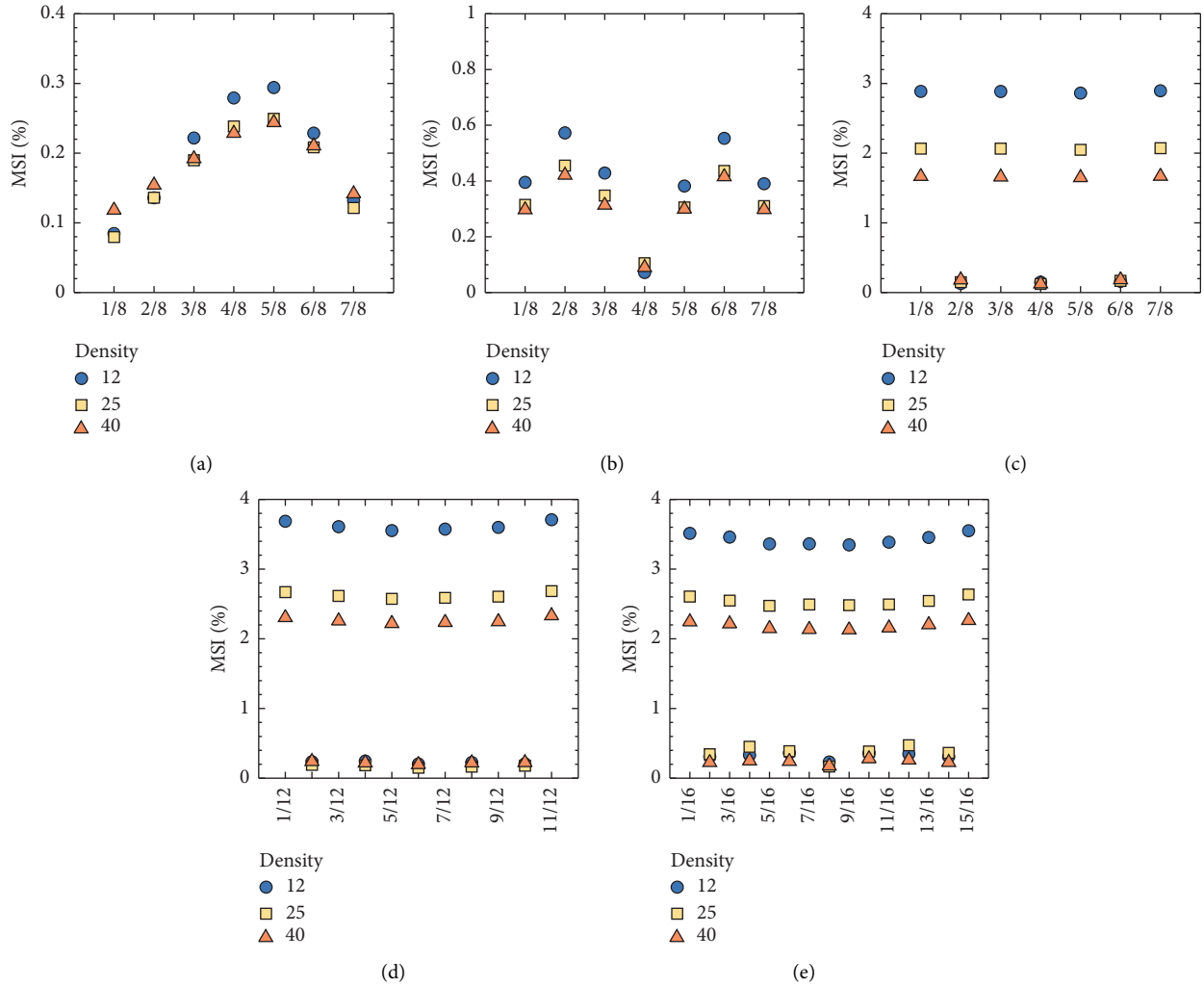


FIGURE 11: MSIs of pedestrians standing on different locations under different VIV frequencies and traffic densities: (a) $f=0.101$ Hz; (b) $f=0.128$ Hz; (c) $f=0.242$ Hz; (d) $f=0.378$ Hz; (e) $f=0.531$ Hz.

$f=0.378$ Hz, three whole waves can be observed for the first main span, so the 1/12, 3/12, 5/12, 7/12, 9/12, and 11/12 span locations represent wave crests/troughs, and 2/12, 4/12, 6/12, 8/12, and 10/12 span locations are the nodes of the VIV wave.

The results in Figure 11 imply that the standing location of the pedestrian has a significant influence on the associated MSI. Generally, this is related to the wave amplitude in terms of the VIV mode shape at the specific location, and the pedestrian standing on the wave crest/trough points has a relatively large MSI. For the example in Figure 11(a), the MSIs for pedestrians standing on 1/8, 2/8, 3/8, and 4/8 span locations under the busy traffic flow are 0.12%, 0.15%, 0.19%, and 0.23%, respectively. The increasing traffic density is found to also be able to reduce the MSI, particularly for standing locations with relatively large wave amplitudes. For the example in Figure 11(d), the MSIs for pedestrians standing on the 1/12 span location under free, moderate, and busy traffic flows are 3.69%, 2.67%, and 2.31%, respectively. To comprehensively

understand the influence of traffic density, PSDs of the vertical bridge acceleration at the 1/12 span location under different traffic densities and VIV amplitudes for VIV frequency = 0.378 Hz are presented in Figure 12. It can be seen that a larger traffic density can result in a significantly smaller maximum PSD, and an increasing VIV amplitude can amplify the PSD. For instance, the maximum PSDs for VIV frequency = 0.378 Hz and VIV amplitude = 0.3 m under free, moderate, and busy traffic flows are 0.84, 0.62, and 0.43 m^2/s^3 , respectively; as the VIV amplitude increases to 0.9 m, the maximum PSDs for free, moderate, and busy traffic flows become 2.54, 1.88, and 1.31 m^2/s^3 . This phenomenon can be attributed to the additional structural damping introduced by the increasing vehicles, which causes a smaller VIV amplitude given the same VIV event. Besides, one can observe that the vehicle rider's feeling on VIVs remains worse than the pedestrian's feeling because the mean MSI for sedan car drivers under the same VIV event and free traffic flow as shown in Figure 11(d) is 3.94%.

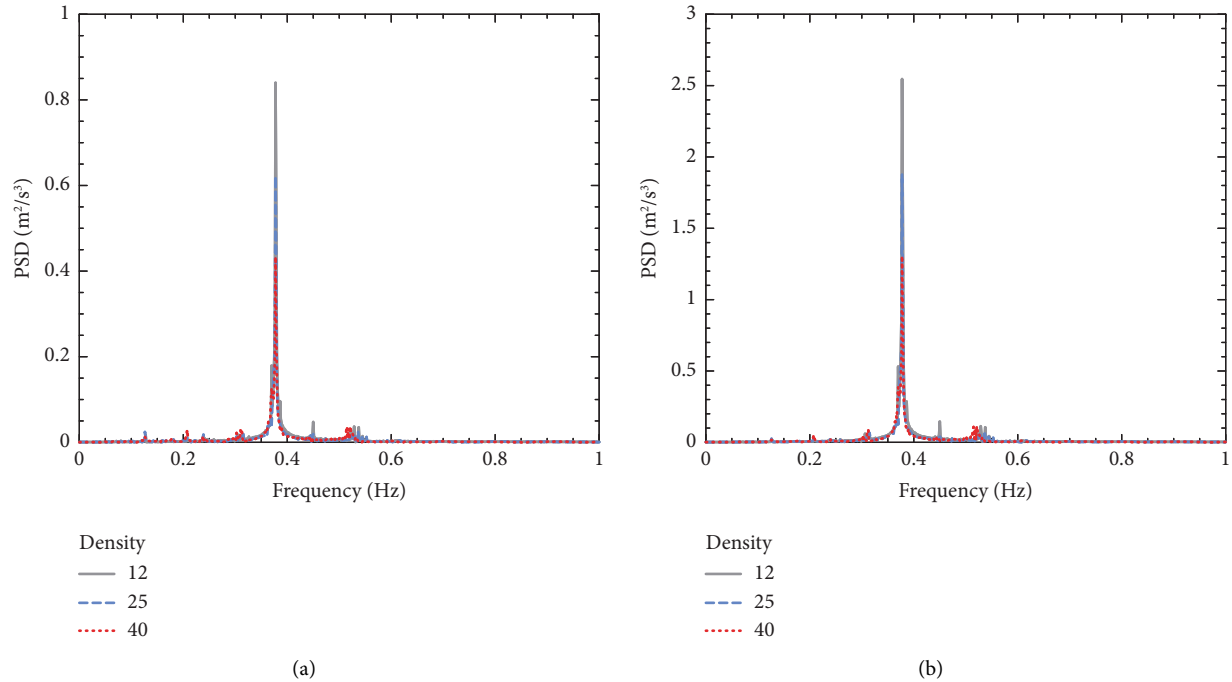


FIGURE 12: PSDs of the vertical bridge acceleration at the 1/12 span location under different traffic densities and VIV amplitudes: (a) VIV amplitude = 0.3 m; (b) VIV amplitude = 0.9 m.

5. Concluding Remarks

This study attempts to revisit the serviceability issue of long-span bridges (LSBs) under vortex-induced vibrations (VIVs) based on bridge users' feelings, which are usually characterized by human body vibration. An evaluation framework of human body vibration is proposed in the context of a wind-traffic-bridge system, particularly designed for LSBs experiencing VIVs. Notably, this study advocates using the motion sickness index (MSI) to study the influence of VIVs rather than the currently popular human comfort index, and the human body vibration assessment method for a standing person (e.g., pedestrian on the bridge) is introduced. Several case studies are performed to comprehensively examine the bridge users' feelings on VIVs based on a prototype long-span suspension bridge. The major findings are summarized as follows:

- (1) The vehicle vibration is closely related to and typically more significant than the bridge vibration, which is dominated by the VIV and vehicle-bridge interaction (VBI) in the current context. The VIV mainly causes vehicle vibration in a low frequency range (typically below 0.5 Hz), and the VBI can excite the vehicle vibration in a relatively high frequency range (e.g., above 3 Hz).
- (2) Using the OVTV (human comfort index) is suitable to distinguish the effect of road roughness on bridge users' feelings, while the potential serviceability issue caused by VIVs might be neglected. Nevertheless, using the MSI can obviously identify the serviceability issue for LSBs under VIVs. These are because

OVTV and MSI are concerned with human body vibration with different frequency contents. By using the MSI, one can filter out the influence of VBI and road roughness to a large extent, only focusing on the vibration content in the VIV-sensitive range. On the contrary, using the human comfort index can filter out the influence of VIV.

- (3) The MSI of vehicle riders is typically slightly larger than that of pedestrians, resulting in a worse feeling on VIVs. The influence of VIV amplitude on MSI is intuitive, i.e., a larger VIV amplitude always causes a larger MSI (worse bridge serviceability). The influence of VIV frequency on MSI is more complex: a higher VIV frequency leads to a more significant human body vibration, but after the frequency weighting in calculating MSI, such a more significant human body vibration does not necessarily produce a larger MSI.
- (4) For the real-world engineering practice involving stochastic traffic loading, it is found that traffic loads can mitigate the adverse effect of VIVs on MSI (or bridge serviceability). As the traffic density on the bridge increases, the associated MSI for bridge users often becomes smaller. This phenomenon can be explained by the remarkable damping deduced from multiple vehicles.
- (5) For the pedestrians on the bridge, their feelings (or MSI) are highly dependent on their standing locations. Generally, this is related to the wave amplitude in terms of the VIV mode shape at the specific location, and the pedestrian standing on the wave

crest/trough points has a relatively large MSI. Moreover, the increasing traffic density on the bridge is found to be able to reduce the associated MSI, especially when involving standing locations with relatively large wave amplitudes.

Despite the potential merits, future efforts are recommended to incorporate an advanced vortex-induced force (VIF) model that can well characterize aerodynamic damping behaviors (e.g., [30]). Such efforts are especially inducive for practical applications requiring accurate quantitative results (e.g., conducting traffic management for LSBs under VIVs). Nevertheless, the major findings of this study are expected to be free from the influence of a different VIF model because they are basically qualitative insights related to the VIV frequency. Meanwhile, the pedestrian's feeling is only assessed for persons standing at a constant point, considering most pedestrians on LSBs are specialized workers rather than regular pedestrians, and these workers mostly stay at a constant location to finish their assignments. Nevertheless, further endeavors can be made to perform human-structure interaction analyses [31] to study the feelings of pedestrians walking through the bridge. Moreover, the temperature effect [8, 32] is worth considering to accurately simulate the VIV event as well as provide predictive user's feeling assessments. In addition, the risk of single-vehicle crashes [33] on LSBs under VIVs is worth studying, given such a comprehensive modeling framework. Finally, the bridge users' MSI can be assessed from monitoring data as a supplement for the current numerical study, in which one may need to carefully deal with real-world disturbances in the collected vibration signal. In that case, some prior knowledge about the inherent physics and signal-processing techniques might be helpful [34, 35].

Data Availability

All data, models, or codes that support the findings of this study are available upon reasonable request.

Disclosure

Any opinions, findings, and conclusions expressed in this material are those of the investigators and do not necessarily reflect the views of the sponsor.

Conflicts of Interest

The authors declare that they have no conflicts of interest.

Acknowledgments

The authors gratefully acknowledge the support of this research by National Natural Science Foundation of China (grant nos. 52278532 and 51908472), Natural Science Foundation of Sichuan Province (24NSFSC1567), and China Postdoctoral Science Foundation (grant nos. 2019TQ0271 and 2019M663554). The support is greatly appreciated.

References

- [1] E. Simiu and D. Yeo, *Wind Effects on Structures: Modern Structural Design for Wind*, John Wiley & Sons, Hoboken, NJ, USA, 2019.
- [2] A. Kareem and Y. Tamura, *Advanced Structural Wind Engineering*, Springer, Singapore, 2013.
- [3] Y. C. Hwang, S. Kim, and H.-K. Kim, "Cause investigation of high-mode vortex-induced vibration in a long-span suspension bridge," *Structure and Infrastructure Engineering*, vol. 16, no. 1, pp. 84–93, 2020.
- [4] Y.-L. Xu, *Wind Effects on cable-supported Bridges*, John Wiley & Sons, Hoboken, NJ, USA, 2013.
- [5] Y. Yang, T. Ma, and Y. Ge, "Evaluation on bridge dynamic properties and VIV performance based on wind tunnel test and field measurement," *Wind and Structures*, vol. 20, no. 6, pp. 719–737, 2015.
- [6] T. Argentini, D. Rocchi, and A. Zasso, "Aerodynamic interference and vortex-induced vibrations on parallel bridges: the Ewijk bridge during different stages of refurbishment," *Journal of Wind Engineering and Industrial Aerodynamics*, vol. 147, pp. 276–282, 2015.
- [7] F. Weber and M. Mašlanka, "Frequency and damping adaptation of a TMD with controlled MR damper," *Smart Materials and Structures*, vol. 21, no. 5, Article ID 55011, 2012.
- [8] H.-W. Zhao, Y.-L. Ding, A.-Q. Li, X.-W. Liu, B. Chen, and J. Lu, "Evaluation and early warning of vortex-induced vibration of existed long-span suspension bridge using multi-source monitoring data," *Journal of Performance of Constructed Facilities*, vol. 35, no. 3, Article ID 4021007, 2021.
- [9] J. Zhang, L. Zhou, Y. Tian, S. Yu, W. Zhao, and Y. Cheng, "Vortex-induced vibration measurement of a long-span suspension bridge through noncontact sensing strategies," *Computer-Aided Civil and Infrastructure Engineering*, vol. 37, no. 12, pp. 1617–1633, 2022.
- [10] L. Zhao, C. Liu, and Y. Ge, "Vortex-induced vibration sensitivity of bridge girder structures (in Chinese)," *Acta Aerodynamica Sinica*, vol. 38, pp. 694–704, 2020.
- [11] J. Zhu, Z. Xiong, H. Xiang, X. Huang, and Y. Li, "Ride comfort evaluation of stochastic traffic flow crossing long-span suspension bridge experiencing vortex-induced vibration," *Journal of Wind Engineering and Industrial Aerodynamics*, vol. 219, Article ID 104794, 2021.
- [12] D. Dan, X. Yu, F. Han, and B. Xu, "Research on dynamic behavior and traffic management decision-making of suspension bridge after vortex-induced vibration event," *Structural Health Monitoring*, vol. 21, no. 3, pp. 872–886, 2022.
- [13] Aashto, *AASHTO LRFD Bridge Design Specifications*, Aashto, Washington, DC, USA, 2020.
- [14] Ministry of Transportation and Communication of PRC, "Jtg/T3360-01-2018 Wind resistance design guideline for highway bridges," China Communications Press Co Ltd, Beijing, China, 2018.
- [15] H. Sato, "Wind-resistant design manual for highway bridges in Japan," *Journal of Wind Engineering and Industrial Aerodynamics*, vol. 91, no. 12-15, pp. 1499–1509, 2003.
- [16] H. Yu, B. Wang, G. Zhang, Y. Li, and X. Chen, "Ride comfort assessment of road vehicle running on long-span bridge subjected to vortex-induced vibration," *Wind and Structures*, vol. 31, pp. 393–402, 2020.
- [17] G.-Q. Zhang, B. Wang, Q. Zhu, and Y.-L. Xu, "Dynamic behavior and ride comfort of a vehicle moving on a long suspension bridge within multi-mode lock-in regions,"

- Journal of Wind Engineering and Industrial Aerodynamics*, vol. 234, Article ID 105345, 2023.
- [18] International Organization for Standardization, *2631-1: Mechanical Vibration and Shock-Evaluation of Human Exposure to Whole-Body Vibration*, ISO, Geneva, Switzerland, 1997.
- [19] Z. Xiong, J. Zhu, K. Zheng, W. Zhang, Y. Li, and M. Wu, "Framework of wind-traffic-bridge coupled analysis considering realistic traffic behavior and vehicle inertia force," *Journal of Wind Engineering and Industrial Aerodynamics*, vol. 205, Article ID 104322, 2020.
- [20] H. Ruscheweyh and G. Sedlacek, "Crosswind vibrations of steel stacks.-critical comparison between some recently proposed codes," *Journal of Wind Engineering and Industrial Aerodynamics*, vol. 30, no. 1-3, pp. 173-183, 1988.
- [21] C. Cai and S. Chen, "Framework of vehicle-bridge-wind dynamic analysis," *Journal of Wind Engineering and Industrial Aerodynamics*, vol. 92, no. 7-8, pp. 579-607, 2004.
- [22] C. J. Baker, "A simplified analysis of various types of wind-induced road vehicle accidents," *Journal of Wind Engineering and Industrial Aerodynamics*, vol. 22, no. 1, pp. 69-85, 1986.
- [23] S. Chen and J. Wu, "Modeling stochastic live load for long-span bridge based on microscopic traffic flow simulation," *Computers & Structures*, vol. 89, no. 9-10, pp. 813-824, 2011.
- [24] J. Zhu, W. Zhang, and M. Wu, "Coupled dynamic analysis of the vehicle-bridge-wind-wave system," *Journal of Bridge Engineering*, vol. 23, no. 8, Article ID 4018054, 2018.
- [25] Y. Zhou and S. Chen, "Vehicle ride comfort analysis with whole-body vibration on long-span bridges subjected to crosswind," *Journal of Wind Engineering and Industrial Aerodynamics*, vol. 155, pp. 126-140, 2016.
- [26] K. C. S. Kwok, P. A. Hitchcock, and M. D. Burton, "Perception of vibration and occupant comfort in wind-excited tall buildings," *Journal of Wind Engineering and Industrial Aerodynamics*, vol. 97, no. 7-8, pp. 368-380, 2009.
- [27] International Organization for Standardization, *Mechanical Vibration—Road Surface Profiles—Reporting of Measured Data*, ISO, Geneva, Switzerland, 1995.
- [28] Y. Yang and K. Chang, "Extracting the bridge frequencies indirectly from a passing vehicle: parametric study," *Engineering Structures*, vol. 31, no. 10, pp. 2448-2459, 2009.
- [29] J. Zhu, S.-J. Jiang, Z. Xiong, M. Wu, and Y. Li, "Longitudinal vibration control strategy for long-span suspension bridges under operational and extreme excitations using eddy current dampers," *Structures*, vol. 58, Article ID 105603, 2023.
- [30] M. Zhang, F. Xu, and O. Øiseth, "Aerodynamic damping models for vortex-induced vibration of a rectangular 4:1 cylinder: comparison of modeling schemes," *Journal of Wind Engineering and Industrial Aerodynamics*, vol. 205, Article ID 104321, 2020.
- [31] J. W. Qin, S. S. Law, Q. S. Yang, and N. Yang, "Pedestrian-bridge dynamic interaction, including human participation," *Journal of Sound and Vibration*, vol. 332, pp. 1107-1124, 2013.
- [32] H. Zhao, Y. Ding, L. Meng, Z. Qin, F. Yang, and A. Li, "Bayesian multiple linear regression and new modeling paradigm for structural deflection robust to data time lag and abnormal signal," *IEEE Sensors Journal*, vol. 23, no. 17, pp. 19635-19647, 2023.
- [33] Z. Xiong and S. Chen, "A multi-fidelity approach for reliability-based risk assessment of single-vehicle crashes," *Accident Analysis & Prevention*, vol. 195, Article ID 107391, 2024.
- [34] X. Zhang, Y. Ding, H. Zhao et al., "Mixed skewness probability modeling and extreme value predicting for physical system input-output based on full bayesian generalized maximum-likelihood estimation," *IEEE Transactions on Instrumentation and Measurement*, vol. 73, pp. 1-16, 2024.
- [35] H. Zhao, Y. Ding, A. Li, B. Chen, and X. Zhang, "State-monitoring for abnormal vibration of bridge cables focusing on non-stationary responses: from knowledge in phenomena to digital indicators," *Measurement*, vol. 205, Article ID 112148, 2022.